



Removal of nitrate from drinking water by adsorption using ion exchange resin

Chabani Malika^a, Akhrib Kenza^a, Ait Ouaisa Yasmine^a, Amrane Abdeltif^{bc,*}, Bensmaili Aicha^a

^aLaboratoire de Génie de la Réaction, Faculté de Génie des Procédés et Génie Mécanique U.S.T.H.B. BP 32, El Allia, Bab Ezzouar, Algérie

^bEcole Nationale Supérieure de Chimie de Rennes, CNRS, UMR 6226, Avenue du Général Leclerc, CS 50837, 35708 Rennes Cedex 7, France

^cUniversité européenne de Bretagne, 5 Bd Laënnec, 35000 Rennes, France

Tel. +33223238155; Fax +33223238120; email: abdelatif.amrane@univ-rennes1.fr.

Received 31 August 2009; accepted 23 May 2010

ABSTRACT

Ion exchange technology is currently the best way to remove nitrate from drinking water. A commercial resin was tested to examine the effectiveness of adsorption for nitrate removal; the resin is Amberlite IRA 400, since it is considered the most promising owing to its chemical stability and ability to control surface chemistry. KNO₃ solution (22.15 mg L⁻¹) was used in batch adsorption experiments. Adsorbent dosages were varied from 0.875 to 5 g L⁻¹. An increase in adsorbent dosage increased the percent removal of nitrate. The retention was initially very fast and maximum retention was observed within 30 min of agitation. Two simplified kinetic models were considered to investigate the ion exchange mechanisms, i.e. the liquid film diffusion and the intraparticle diffusion models, and it was shown that the former controlled the beginning of the process while the latter predominated at the end of the process.

Keywords: Adsorption; Ion-exchange resins; Kinetic models; Nitrate removal

1. Introduction

The nitrate in groundwater used for drinking in rural areas is becoming an important problem due to its harmful effects. Among several techniques available for the removal of nitrate, such as ion exchange, biological denitrification, chemical reduction and electro dialysis, the ion exchange process seems to be the most suitable for small water suppliers contaminated by nitrate because of its simplicity, effectiveness and relatively low cost [1, 2]. Adsorption on resin is considered as the most promising method owing to its

chemical stability and ability to control surface chemistry [3], Amberlite IRA 400 contains an amine group, which is particularly reactive and able to retain anions [4, 5]; these strong base anion exchangers have a significantly stronger affinity for nitrates [6].

To understand the dynamic interactions of nitrate with resins and to predict their fate with time, knowledge concerning the kinetics of these processes is important [7]. A number of models have been suggested in the literature for simulation of the adsorption experimental data.

Various mechanisms and steps in ion-exchange phenomena can control the kinetics. Four major rate-limiting steps are generally cited [8,9]: (1) mass transfer

*Corresponding author

of solute from solution to the boundary film; (2) mass transfer of solute from boundary film to surface; (3) sorption and ion exchange of ions onto sites; (4) internal diffusion of solute. The third step is assumed to be very rapid and non-limiting in this kinetic analysis: sorption is a rapid phenomenon. The first and the second steps are external mass transfer resistance steps, depending on various parameters such as agitation and homogeneity of solution. The fourth one is an internal particle diffusion resistance step. Effective design and scale-up procedures require a good theoretical understanding of both thermodynamics and kinetics of ion exchange processes, with particular reference to models accounting for mass transfer in the solid phase and in the liquid phase. This paper reviews kinetics of ion exchange with mass transfer as the rate-controlling step. The objective was to demonstrate the importance of the mass transfer in ion exchange kinetics by modelistic approach. In this aim, two simplified kinetic models were considered:

The intraparticle diffusion equation

The intraparticle diffusion model is a single-resistance model in nature and can be derived from Fick's second law under two assumptions [10]: first, the intraparticle diffusivity D is constant; secondly, the uptake of sorbate by the adsorbent is small relative to the total quantity of sorbate present in the solution. Thus, the mathematical expression obtained for the intraparticle diffusion model is:

$$q_t = k_p t^{0.5} + C, \quad (1)$$

Where C is the intercept and k_p ($\text{mg/g}\cdot\text{min}^{-0.5}$) is defined as the intraparticle diffusion rate constant

According to this model (eq. 1), the plot of uptake, q_t , versus the square root of time ($t^{1/2}$) should be linear if intraparticle diffusion is involved in the adsorption process and if these lines pass through the origin then intraparticle diffusion is the rate-controlling step. When the plots do not pass through the origin, it is indicative of some degree of boundary layer control showing that the intraparticle diffusion is not the only rate-limiting step, but also other kinetic models may control the rate of adsorption, all of which may be operating simultaneously. The slope of the linear portion from the figure can be used to derive values for the rate parameter, k_p , for the intraparticle diffusion; k_p has been widely used to determine the intraparticle diffusion coefficients D [11-13].

The values of the diffusion coefficient largely depend on the surface properties of adsorbents. The diffusion coefficients for the intraparticle transport

have been calculated at different resin doses and various concentrations by employing Eq. (2):

$$D = \frac{\pi}{36} \left(k_p \frac{d}{q_e} \right)^2 \quad (2)$$

Where d is the mean particle diameter (cm), D is the intraparticle diffusion coefficient (cm^2/s) and q_e the amount adsorbed at equilibrium (mg/g).

The liquid film diffusion equation [14,15]

According to Boyd et al. [15], from the linear relationship of $\text{Ln}(1-F)$ vs t it can be deduced that the liquid film spreading is the predominating step of the adsorption process [16].

$$\text{Ln}(1 - F) = -kt \quad (3)$$

Where F is the fractional attainment of equilibrium (q_t/q_e) and k is the film diffusion rate constant (min^{-1}). A linear plot of $\text{Ln}(1-F)$ versus t with zero intercept would suggest that the kinetics of the sorption process is controlled by the diffusion through the liquid film surrounding the solid sorbents.

(c) Diffusion-controlled kinetic models

An understanding of the significance of diffusion mechanisms and accurate estimates of the diffusivities of the adsorbent particles are determined from the diffusion controlled kinetic models based on the interpretation of experimental data. Adsorbate transport from the solution phase to the surface of the adsorbent particles occurs in several steps. The overall adsorption process may be controlled by one or more steps, e.g. film or external diffusion, pore diffusion, surface diffusion and adsorption on the pore surface, or a combination of more than one step.

The Biot number (eq. 4) is the ratio of the rates of external mass transfer to internal mass transfer. Its value indicates which transfer determines the adsorption rate. For $\text{Biot} \rightarrow \infty$ (greater than 100), the mass transfer rate to the particle surface is very high. In this case, close concentrations on the interfacial surface and the particle surface are recorded; the major resistance is within the adsorbent particle rather than external to the particle [17]. For small Biot values = 0.1-1.0, the adsorption rate is determined by the external diffusion.

$$\text{Bi} = \frac{k_f d}{D} \quad (4)$$

k_f is the external mass transfer coefficient (cm/s).

The mass transport through a film determines the mass transfer coefficient k_f in the liquid phase. The boundary model assumes that the surface concentration of nitrates, C_i , is negligible at $t=0$, and consequently intraparticle diffusion is negligible. Change in nitrates concentration with respect to time is related to the liquid–solid mass transfer coefficient, k_f , through equation (5) [18,19]:

$$\frac{dC}{dt} = k_f A/V(C - C_i) \quad (5)$$

In the initial stage of the process, the adsorbate concentration in the particle is nil. With a lack of concentration gradient inside the particle, mass transport corresponds exclusively to mass transfer to the external surface of the adsorbent through a laminar layer surrounding the particle. Initially, only the mass transfer from the liquid to the particle surface limits the mass transfer rate, which is therefore determined by the mass transfer coefficient through a laminar layer surrounding the particle:

$$\left[\frac{dC/C_0}{dt} \right]_{t=0} = k_f A/V \quad (6)$$

Where C_0 , C , A/V and t are the initial ion concentration and its concentration at a given time t , the total interfacial area of the particles (cm^2) to the total solution volume (cm^3), and the adsorption time, respectively.

A/V is expressed as:

$$\frac{A}{V} = \frac{3M}{\rho d} \quad (7)$$

Where M is the adsorbent dosage (g/cm^3) and ρ the apparent density of the adsorbent (g/cm^3). If film diffusion was to be the rate-determining step in the adsorption of nitrates on the surface of the resin, the value of the film diffusion coefficient (k_f) should be in the range 10^{-6} to 10^{-8} cm/s [20].

2. Experimental

The kinetic experiments were performed in static conditions at room temperature. The bath method was used for kinetic measurements and performed as follows: in a glass vessel, samples of the resins in the swelling form were contacted with 0.8 L KNO_3 aqueous solution of known concentration. At known time intervals the concentrations of NO_3^- anions in the aqueous solution was determined. The concentration of residual nitrate ions was determined spectrophotometrically according to the Rodier protocol [21] using a Jenway 6105 model UV/visible spectrophotometer.

Table 1

General description and some properties of Amberlite IRA 400

Ionic form	Cl^-
Functional group	$-\text{N}^+\text{R}_3$
Polymer Matrix	Polystyrene-divinylbenzene
Structure	Gel type beads
pH range	0 - 14
Effective size	0.3–0.8 mm
Exchange capacity	2.6–3 eq kg^{-1} of dry mass
Appearance	Yellow to golden spherical beads, translucent
Water retention	42–48%
Visual density in wet state	0.66–0.73 g mL^{-1}
True density in wet state	1.07–1.10 g mL^{-1}
Apparent density (ρ)	1.07 g/cm^3

The sorption capacity q_t (mg g^{-1}) at time t was obtained as follows:

$$q_t = (C_0 - C_t) \frac{v}{m} \quad (8)$$

Where C_0 and C_t (mg L^{-1}) were the liquid-phase concentrations of solutes at the initial and a given time t , respectively, v (L) the volume of solution and m the mass resin (g).

The pH of the aqueous solutions of NO_3^- was approximately 6.8 and did not varied significantly with the dilution.

Before use, the resin was washed in distilled water to remove the adhering dirt and then dried at 50°C . After drying, the resin was screened to obtain a particle size range of 0.3 – 0.8 mm. The main characteristics of the Amberlite IRA 400 are given in table 1.

The stock solution of NO_3^- used in this study was prepared by dissolving an accurate quantity of KNO_3 in distilled water.

3. Results and Discussion

3.1. Effect of the contact time

Fig. 1 shows the effect of the reaction time on the removal of NO_3^- by Amberlite IRA 400. The NO_3^- removal increased with time and achieved equilibrium at about 30 min for 22.15 mg L^{-1} of nitrate concentration used. The percentage of nitrate removal increased rapidly up to approximately 15 min and thereafter, rose slowly before reaching a saturation value in 30 min. A further increase in contact time had a negligible effect on the capacity. The percentage of nitrate removal was higher in the beginning since the surface site initially available for nitrates sorption was very large compared to the concentration of nitrate ions, and

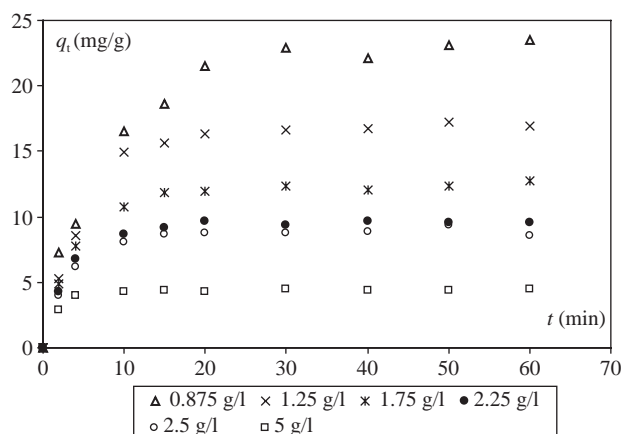


Fig. 1. Effect of the contact time on the adsorption of nitrate sorbed for different resin dosages (pH = 6.8, $C_0 = 22.15 \text{ mg/L}$, $d = 0.715 \mu\text{m}$)

consequently the rate of sorption was very high. However, with increasing coverage the fraction of sorption sites in resin surface rapidly diminished and nitrate ions had to compete among themselves for the sorption sites. This competition led to slow down the interaction and the rate limiting step becomes predominantly dependent on the rate at which nitrate ions were transported from the bulk to the sorbent-adsorbate interface. The kinetics of the interactions was thus likely to be dependent on different rate processes as the interaction time increased [22].

In all subsequent experiments, the equilibrium time was maintained at 60 min, which was considered as sufficient for the removals of nitrate ions. The nitrate ion uptake versus time curves appeared smooth and continuous (Fig. 1) until saturation was achieved.

3.2. Effect of the adsorbent dosage

From the batch experiments, the adsorption yield was determined as follows:

$$\text{Adsorption}(\%) = \frac{(C_0 - C)}{C_0} \cdot 100 \quad (9)$$

The amount of nitrates adsorbed varied with the mass of resin; an increase in resin dosage increased the percent removal of nitrate until a constant level was reached (Fig. 2), in agreement with the available literature [6]. An increase of the resin dosage from 0.875 to 5 g L^{-1} led to an increase of the percentage removal from 88.1% to 95.8%. It was found that the retention of nitrates increased with increasing amount of Amberlite IRA 400 up to 1.40 g (or 1.75 g L^{-1}). This value was taken as the optimum amount. Since the fraction of nitrates removed from the aqueous phase increased as the

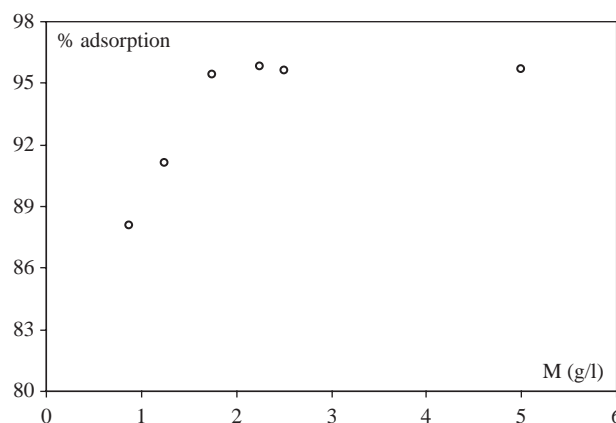


Fig. 2. Effect of adsorbent dosage on the adsorption of nitrates (Adsorption time: 60 min, bead size 0.715 mm)

sorbent dosage was increased in the batch vessel for a fixed initial metal concentration, the curves in Fig. 2 approach asymptotic values from 1.75 to 5.0 g resin L^{-1} . It should however be noted that the specific amount of nitrates adsorbed decreased from 24.7 to 4.54 mg g^{-1} ; This may be attributed to increased adsorbent surface area and the availability of more adsorption sites resulting from the increase of the amount of adsorbent.

Data in Fig. 2 establish that weights of resin higher than 1.75 g L^{-1} are enough to remove almost all nitrates from 22.15 mg L^{-1} solutions at pH 6.8. 1.4 g was chosen as the optimum weight to get the highest mass of loaded nitrates per mass of adsorbent. It should be observed that the adsorption of nitrate on Purolite A 520E resin led to similar results [6].

3.3. Effect of the initial concentration

The effect of the amount of nitrates adsorbed for different initial concentrations onto the ion-exchange resin is presented in Fig. 3. Irrespective of the concentration, adsorption was initially rapid and gradually decreased with the progress of adsorption until reaching the equilibrium. The equilibrium time was found to be 30 min for all concentrations studied. The nitrates removal decreased from 91.9 to 89.7% for increasing nitrate concentrations from 22.15 to 79.7 mg L^{-1} (Fig. 3). Nitrate ions were not completely removed from the aqueous solution at low initial nitrate concentrations. Therefore, the overall adsorption process was affected by external mass transfer diffusion [20]. Nitrates removal was dependent on the initial concentration since the amount adsorbed increased for increasing initial concentrations. The C_0 provided the necessary driving force to overcome the resistance to the mass transfer of nitrates between the aqueous and the solid phases. The increase in C_0 also enhanced the

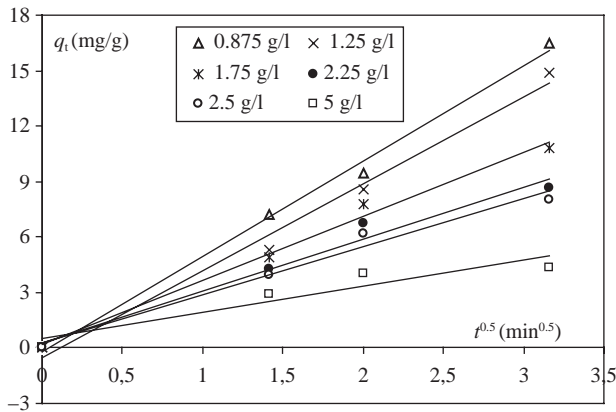


Fig. 3. Effect of initial concentration on the removal of nitrates. (pH = 6.8, M = 1.25g/L, d = 0.565µm)

interaction between nitrates and resin, and hence enhanced the adsorption uptake of nitrates.

3.4. Kinetic models

The plot of q_t , the amount of adsorbate adsorbed per unit weight of adsorbent versus the square root of time has been commonly used to describe an adsorption process controlled by the diffusion in the adsorbent particle and the consecutive diffusion in the bulk of the solution [23].

According to the Intraparticle diffusion model (Eq. 1), a linear plot of the average particle uptake, q_t , versus the square root of time ($t^{1/2}$) is expected if intraparticle diffusion is involved in the adsorption process and a nil value of the ordinate at the origin indicates that intraparticle diffusion is the rate-controlling step [24].

Figs. 4 and 5 show a plot of $q(t)$ versus $t^{0.5}$ for the experimental results in displayed in Figs. 1 and 3. An apparent linear relationship of $q(t)$ against $t^{0.5}$ was

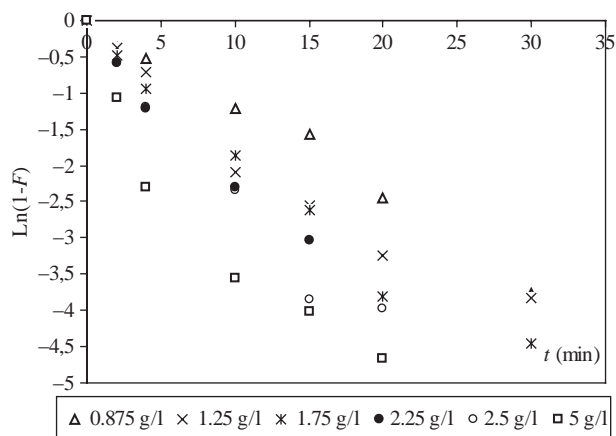


Fig. 4. Test of the intraparticle diffusion kinetic model at different resin dosages

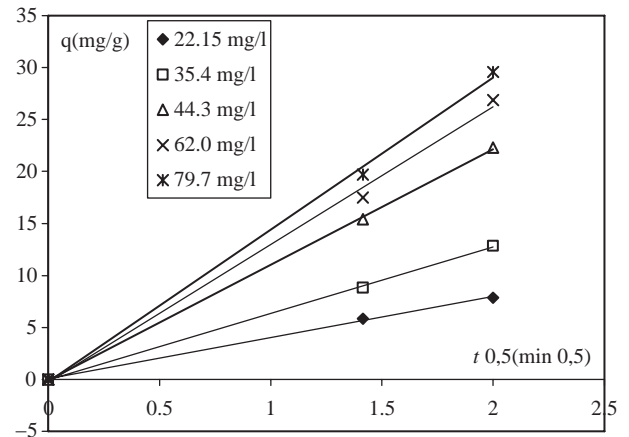


Fig. 5. Test of the intraparticle diffusion kinetic model at different initial concentrations

observed in each case from the beginning to almost the adsorption equilibrium. The intercept at the origin was not nil (Table 2), indicating some degree of boundary layer control. The results suggest the existence and the importance of intraparticle diffusion-controlled mechanism. However, the values of R^2 were found ranging between 0.947 and 0.994. Hence, another mechanism, in addition to the intraparticle diffusion-controlled mechanism, may be expected to play a role in nitrates adsorption onto the resin.

The slope of the linear parts of the curves (Figs. 4 and 5) can be used to derive values for the intraparticle diffusion rate constant, k_p . The intercept C was negative for all experimental conditions and positive for 0.875 to 1.75 g L⁻¹.

Almost all the intercepts reported in the literature are positive, indicating that rapid adsorption occurs within a short period of time [25]. McKay et al. [26,27] have indicated that extrapolating the linear portion of the plot to the axis provides intercepts which are proportional to the extent of the boundary layer thickness. Their experiments were carried out at different mixing intensities, and the obtained intercepts were negative. Thus, they believed that the boundary layer thickness retarded intraparticle diffusion. To our knowledge the negative intercepts have never been discussed.

The intraparticle diffusion model for nitrates adsorption shows that the initial adsorption was absent in the range of concentrations studied (0.875 to 1.75 g L⁻¹). For the other experimental conditions the positive intercept values indicated a large initial adsorption which becomes more important for high resin doses. A non-nil value for the origin intercept indicates an initial boundary layer resistance.

A liquid film diffusion process controlling the rate of adsorption was examined by plotting the time-

Table 2

Constant rates for removal of nitrates with Amberlite IRA 400 resin at different adsorbent dosages and different initial concentrations

	Intraparticle diffusion			Film diffusion	
	R^2	$C(\text{mg}\cdot\text{g}^{-1})$	$k_p (\text{mg g}^{-1} \text{min}^{-0.5})$	R^2	Kinetic constant $k (\text{min}^{-1})$
$M (\text{g/l})$					
0.875	0.994	-0.182	4.86	0.991	0.121
1.25	0.981	-0.555	4.32	0.981	0.135
1.75	0.983	-0.166	2.89	0.987	0.145
2.25	0.947	0.302	2.43	0.981	0.199
2.5	0.950	0.276	2.40	0.992	0.246
5	0.816	0.496	1.12	0.998	0.573
$C_o(\text{mg/l})$					
22.15	0.9983	-0.055	3.97	0.9875	0.135
35.4	0.9995	-0.050	6.39	0.9943	0.141
44.3	0.9997	-0.069	11.1	0.9968	0.171
62.0	0.9961	-0.280	13.2	0.9933	0.180
79.7	0.9980	-0.221	14.6	0.9976	0.172

course of $\text{Ln}(1-F)$ for 30 minutes of contact time; and the film diffusion rate constant k corresponded to the linear part of the plot. Fig. 6 shows a plot of $\text{Ln}(1-F)$ versus t and an apparent linear relationship was observed from the beginning to 30 min for resin doses of 0.875, 1.25 and 1.75 g L^{-1} . For other resin doses (*i.e.* 2.25 and 2.5), the linearity ceased at 15 min and for 5 g L^{-1} the line ceased to deviate from linearity after 5 min. For various initial nitrate concentrations the linear relationship was observed for the first 20 min of experiment (Fig. 7). The intercepts were close to zero.

The results suggest the existence and the importance of film diffusion-controlled transport mechanism in nitrates adsorption onto resin. The short period of film diffusion for great resin dose was most likely due

to initial adsorption as shown with intraparticle diffusion model.

Beyond 30 min or 20 min the plot of $\text{Ln}(1-F)$ versus time is not linear any more, indicating that the liquid film diffusion is not only the predominant mechanism for nitrates adsorption on Amberlite IRA 400. The external mass transfer dominates the beginning of the process.

The results show that intraparticle diffusion and film diffusion models were valid for the considered system. All the correlation coefficients obtained were higher than 0.96. The adsorption of nitrates onto the Amberlite IRA 400 resin can be considered to be a process controlled by both film and intraparticle diffusion limited mechanisms.

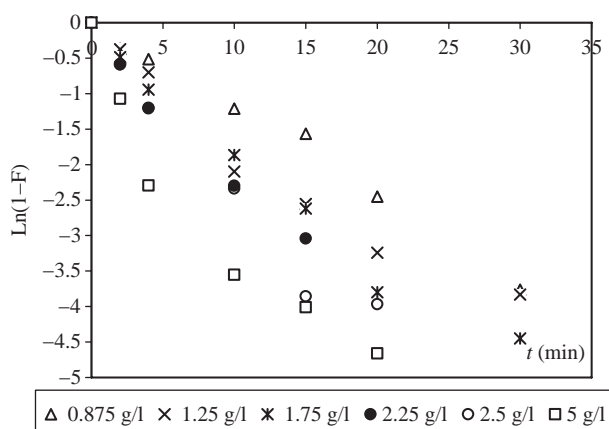


Fig. 6. Test of the liquid film diffusion kinetic model at different resin dosages

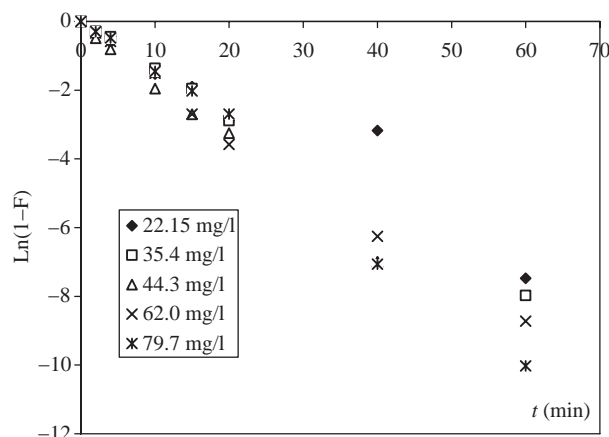


Fig. 7. Test of the liquid film diffusion kinetic model at different initial concentrations

Table 3

The adsorption diffusion kinetic parameters of nitrates on the resin at different initial concentrations and adsorbent dosages

	$k_p(\text{mg/g}\cdot\text{min}^{0.5})$	$k_f(\text{cm}/\text{min})$	$D(\text{cm}^2/\text{min})$	Biot
$M(\text{g}/\text{L})$				
0.875	4.86	1.394	$2.98 \cdot 10^{-6}$	26438.9
1.25	4.32	1.331	$4.51 \cdot 10^{-6}$	16674.4
1.75	2.89	0.833	$3.58 \cdot 10^{-6}$	13131.8
2.25	2.43	0.888	$4.46 \cdot 10^{-6}$	11244.3
2.5	2.40	0.109	$5.44 \cdot 10^{-6}$	1132.07
5	1.12	1.153	$4.41 \cdot 10^{-6}$	14765.3
$C_o(\text{mg}/\text{L})$				
22.15	3.97	1.26	$4.51 \cdot 10^{-6}$	19240.5
35.4	6.39	1.01	$2.24 \cdot 10^{-6}$	25475.4
44.3	11.1	0.97	$5.33 \cdot 10^{-6}$	10282.4
62.0	13.2	0.94	$3.26 \cdot 10^{-6}$	16291.4
79.7	14.6	0.74	$2.47 \cdot 10^{-6}$	16927.1

Kinetic parameters and correlation coefficients obtained by the two models are given in table 2. Table 2 shows the dependence of the rate constants k_p and k on the resin dosages. The values of k_p decreased and the values of k increased for increasing adsorbent dosages. The reverse effect of the adsorbent dosages on k_p was also reported for other adsorption systems [7], though no explanation was provided.

The constant rate values k_p increased from 3.97 to $14.6 \text{ mg g}^{-1} \text{ min}^{-1/2}$ for initial nitrate concentrations increasing from 22.15 to 79.7 mg L^{-1} . Hence, nitrate concentrations in the solution had a strong influence on both the adsorption diffusion kinetics and the mechanism controlling the kinetic coefficient. At high initial concentrations, the gradient generated between the solution and the centre of the particles led to enhanced nitrates diffusion through the film surrounding the particle and into the porous structure of the resin.

Diffusion-controlled kinetic models employed for data treatment of kinetic experiments are listed in Table 3. The decrease in the external diffusion coefficients may be attributed to the reduction in the affinity of the external surface towards adsorption [28, 29]. The diffusion coefficients D do not exhibit a distinct dependence on the initial concentration and the resin dose.

The corresponding diffusion coefficients for various concentrations of nitrates and various resin doses varied from 2.24×10^{-6} to $5.44 \times 10^{-6} \text{ cm}^2/\text{min}$. The values of all the Biot numbers obtained in the present study were greater than 100 (Table 3), indicating that the film transfer was not preponderant compared to the intraparticle mass transfer.

4. Conclusion

The adsorption kinetics of nitrates on Amberlite IRA 400 resin as a function of the contact time, the

initial nitrate concentration, and the resin dose was investigated. It was found that the adsorption rate of nitrates on resin increased for increasing initial nitrate concentrations, and resin dose. The kinetic data from experimental investigations have been well described by empirical external mass transfer and intraparticle diffusion models. According to the $t^{0.5}$ test, and the values of the Biot numbers, the result suggests that the rate-controlling mechanism may vary during the course of the sorption process.

Two mechanisms appear to contribute during the process: film diffusion which dominates the beginning of the process, followed by the intraparticle diffusion at the late stage.

References

- [1] K. Mizuta, T. Matsumoto, Y. Hatate, K. Nishihara and T. Nakanishi, Removal of nitrate-nitrogen from drinking water using bamboo powder charcoal, *Bioresour. Technol.*, 95 (2004) 255–257.
- [2] N. Öztürk and T.E. Bektas, Nitrate removal from aqueous solution by adsorption onto various materials, *J. Hazard. Mater.*, B112 (2004) 155–162.
- [3] N.I. Chubar, V.F. Samanidou, V.S. Kouts, G.G. Gallios, V.A. Kanibolotsky, V.V. Strelko and I.Z. Zhuravlev, Adsorption of fluoride, chloride, bromide, and bromate ions on a novel ion exchanger, *J. Colloid Interf. Sci.*, 291 (2005) 67–74.
- [4] G.A.F. Roberts and K.E. Taylor, Chitosan gels-3: the formation of gels by reaction of chitosan with glutaraldehyde, *Makromol. Chem.*, 190 (1989) 951–960.
- [5] H. Yoshida, H. Kishimoto and T. Kataoka, Adsorption of strong acid on polyaminated highly porous chitosan: equilibria, *Ind. Eng. Chem. Res.*, 33 (1994) 854–859.
- [6] S. Samatya, N. Kabay, Ü. Yüksel, M. Arda and M. Yüksel, Removal of nitrate from aqueous solution by nitrate selective ion exchange resins, *React. Funct. Polym.*, 66 (2006) 1206–1214.
- [7] A. Sharma and K.G. Bhattacharyya, *Azadirachta indica* (Neem) leaf powder as a biosorbent for removal of Cd(II) from aqueous medium, *J. Hazard. Mater.*, B125 (2005) 102–112.
- [8] N. Dizgea, E. Demirbasb, M. Kobayaa, Removal of thiocyanate from aqueous solutions by ion exchange, *J. Hazard. Mater.*, 166 (2009) 1367–1376.

- [9] G.C. Lee, G. L. Foutch, A. Anmachalam An evaluation of mass-transfer coefficients for new and used ion-exchange resins. *React. Funct. Polym.*, 35 (1997) 55–73.
- [10] X. Yang and B. Al-Duri, Kinetic modeling of liquid-phase adsorption of reactive dyes on activated carbon, *J. Colloid. Interf. Sci.*, 287 (2005) 25–34.
- [11] K.H. Choy Keith, J.F. Porter, G. McKay, Intraparticle diffusion in single and multicomponent acid dye adsorption from wastewater onto carbon, *Chem. Eng. J.*, 103 (2004) 133–145.
- [12] T. Kumar Saha, S. Karmaker, H. Ichikawa and Y. Fukumori, Mechanisms and kinetics of trisodium 2-hydroxy-1,1'-azobenzene-3,4'-disulfonate adsorption onto chitosan, *J. Colloid. Interf. Sci.*, 286 (2005) 433–439.
- [13] R. Apiratikul and P. Pavasant, Batch and column studies of biosorption of heavy metals by *Caulerpa lentillifera*, *Bioresour. Technol.*, 99 (2008) 2766–2777.
- [14] F.J. Alguacil, M. Alonso and L.J. Lozano, Chromium (III) recovery from waste acid solution by ion exchange processing using Amberlite IR-120 resin: batch and continuous ion exchange modelling, *Chemosphere*, 57 (2004) 789–793.
- [15] G.E. Boyd, A.M. Adamson and L.S. Myers, The exchange adsorption of ions from aqueous solutions by organic zeolites. II. Kinetics, *J. Amer. Chem. Soc.*, 69 (1949) 2836–2842.
- [16] C.H. Xiong and C.P. Yao, Study on the adsorption of cadmium(II) from aqueous solution by D152 resin. *J. Hazard. Mater.*, 166 (2009) 815–820.
- [17] E. Guibal, C. Milot and J.M. Tobin, Metal–anion sorption by chitosan beads: equilibrium and kinetic studies, *Ind. Eng. Chem. Res.*, 37 (1998) 1454–1463.
- [18] A. Findon, G. McKay and H.S. Blair, Transport studies for the sorption of copper ions by chitosan. *J. Environ. Sci. Health*, A28 (1993) 173–85.
- [19] G. McKay, H.S. Blair and A. Findon, Sorption of metal ions by chitosan. In: Eccles H, Hunt S, editors. *Immobilisation of Ions by Biosorption*. Chichester, UK: Ellis Horwood (1986).
- [20] N. Dizge, E. Demirbas and M. Kobya, Removal of thiocyanate from aqueous solutions by ion exchange, *J. Hazard. Mater.*, 166 (2009) 1367–1376.
- [21] J. Rodier, *Water analysis (in French)*, 7th ed. Dunod, Paris (1996).
- [22] R.R. Sheha and A.A. El-Zahhar, Synthesis of some ferromagnetic composite resins and their metal removal characteristics in aqueous solutions, *J. Hazard. Mater.*, 150 (2008) 795–803.
- [23] M. Chabani, A. Amrane and A. Bensmaili, Kinetic modelling of the adsorption of nitrates by ion exchange resin, *Chem. Eng. J.*, 125 (2006) 111–117.
- [24] J.P. Chen, S. Wu and K.-H. Chong, Surface modification of a granular activated carbon by citric acid for enhancement of copper adsorption, *Carbon*, 41 (2003) 1979–1986.
- [25] W. Feng-Chin, T. Ru-Ling and J. Ruey-Shin, Initial behavior of intraparticle diffusion model used in the description of adsorption kinetics, *Chem. Eng. J.*, 153 (2009) 1–8.
- [26] G. McKay, M.S. Otterburn and A.G. Sweeney, The removal of color from effluent using various adsorbents III silica: rate processes, *Water Res.*, 14 (1980) 15–20.
- [27] G. McKay, The adsorption of dyestuffs from aqueous solutions using activated carbon. III. Intraparticle diffusion process, *J. Chem. Technol. Biotechnol.*, A 33 (1983) 196–204.
- [28] F. Helfferich, *Ion Exchange*, McGraw-Hill, New York (1962).
- [29] M.A.M. Khraisheh, Y.S. Al-Degs, S.J. Allen and M.N. Ahmad, Elucidation of controlling steps of reactive dye adsorption on activated carbon, *Ind. Eng. Chem. Res.*, 41 (2002) 1651–1657.